This is a previous version of the article published in Fuel. 2017, 194: 222-228. doi:10.1016/j.fuel.2017.01.023

# Low temperature glycerol steam reforming on bimetallic PtSn/C catalysts: on the effect of the Sn content

*Laura Pastor-Pérez, Antonio Sepúlveda-Escribano**

Laboratorio de Materiales Avanzados, Instituto Universitario de Materiales de Alicante - Departamento de Química Inorgánica, Universidad de Alicante, Apartado 99, E-03080 Alicante, Spain.

***Corresponding author: Tfn. +34965903974. E-mail: asepul@ua.es**

KEYWORDS: Bimetallic catalysts; PtSn/C; Glycerol steam reforming; Deactivation

ABSTRACT: Steam reforming of glycerol to produce syngas or $H_2$-enriched streams is a promising route that has caught the attention of many researchers around the world. This reaction is typically carried out over metal-based catalysts supported on stable materials. Herein we report a study on the effect of Sn on the catalytic properties of Pt/C in the aforementioned reaction. A series of Pt-Sn/C catalysts with different Pt:Sn ratios were prepared and characterized using ICP, $H_2$-TPR, TEM and XPS techniques, and they were tested in the glycerol steam reforming

reaction at 623 K and atmospheric pressure. The best performance was observed for the catalysts with low tin contents. It was found that Sn promoted oxidation reactions and inhibited methanation. Furthermore, the presence of Sn improved the stability of the catalysts when operating at harsher conditions of temperature and glycerol concentration. A promoter effect of Sn hindering platinum sintering and the formation of coke precursors is proposed as the origin of the observed behaviour.

## 1. Introduction

Fossil fuels are the world's main energy source, but supplies are diminishing while the consumers' demand is progressively growing. In this scenario, there is a need to develop clean and suitable energy alternatives to satisfy the global requirements. Herein, next-generation biofuels, such as biodiesel, have become the most considered substitutes for conventional fossil fuels due to technical, economic, and environmental sustainability.

Biodiesel is comprised of mono-alkyl esters of long-chain fatty acids, which are derived from vegetable oils or animal fats [1-3]. In the biodiesel synthesis process an important amount of glycerol, ca. 10 wt.%, is obtained as by-product. Although glycerol is used as raw material in chemical industry, for instance in food, pharmaceutical, cosmetic, and tobacco industries, the supply of glycerol is larger than the demand due to the increasing biodiesel production. This over stock of glycerol obligates scientific researchers to develop processes which transform it into valuable products and, in this way, to improve the economic viability of the biodiesel production [4,5].

With this perspective, the conversion of glycerol to hydrogen via steam reforming (GSR: glycerol steam reforming) is an interesting alternative [6]. This reaction is very attractive since

glycerol reforming can be performed using well-known technologies, conducted at atmospheric pressure, at relatively low temperatures due to the reactivity of the alcohol, and using conventional fixed-bed reactors [7]. The use of low temperatures during reforming is very interesting because it allows direct coupling (in one reactor) with Fischer-Tropsch (FT) reactions [8] or water-gas shift (WGS) [9]. However, glycerol steam reforming involves complex reactions affecting the hydrogen selectivity and producing high carbon formation rates [10,11].

The glycerol steam reforming reaction can be represented as follows:

$$C_3H_8O_3\ (g) + 3H_2O\ (g) \rightarrow 3CO_2\ (g) + 7H_2\ (g) \qquad \text{Eq.(1)}$$

Thus, it is the combination of two reactions, glycerol decomposition ($C_3H_8O_3\ (g) \rightarrow 3CO\ (g) + 4H_2$) and water-gas shift ($CO\ (g) + H_2O\ (g) \leftrightarrow CO_2\ (g) + H_2\ (g)$).

Many metal catalysts have been reported for the GSR, among which Ru, Rh, Ir, Pd, Pt, Co and mainly Ni are the most representative ones, being the Pt-based catalysts among the most effective for its efficient C-C, O-H and C-H bond cleavages with high activity and selectivity levels [12-14]. The use of bimetallic formulations has been considered as a strategy to enhance the catalytic performance of Pt based catalysts. It is well-established that the second metal may influence the first one through electronic interactions and/or by modifying the morphology of the active sites. Among the metallic promoters, Sn is one of the most preferable options. Sn addition as promoter of catalytic activity and selectivity has been extensively studied in reactions such as hydrogenations in the field of fine chemistry, alkane dehydrogenation and methane reforming. In all the cases it has been observed that Sn addition improves significantly the catalyst activity, selectivity and/or stability [15, 16].

The nature of the support influences the catalytic performance of the catalysts in steam reforming reactions. Catalysts with Pt supported on $Al_2O_3$, $ZrO_2$, $CeO_2/ZrO_2$, $MgO/ZrO_2$ and carbon have been studied, and it was found that the oxide-supported systems are deactivated during the reaction, while carbon-supported catalysts showed a stable conversion of glycerol to synthesis gas for at least 30 hours [6]. High levels of unsaturated hydrocarbons such as ethylene were found in the gas stream of the catalyst suffering a more rapid deactivation. These unsaturated compounds, formed by dehydration reactions on the substrate, are precursors in the formation of coke, and may explain the observed deactivation [17]. Due to its relatively inert chemical nature, carbon does not catalyse such dehydration reactions and, therefore, it exhibits an excellent performance in the reforming of aqueous glycerol solutions. Furthermore, this material has excellent stability under hydrothermal conditions (moderate temperatures and high concentrations of water) [6,18].

In this paper, a series of Pt-Sn/C catalysts with different Sn contents were evaluated in the glycerol steam reforming reaction, in order to determine the effect of tin content on the activity, selectivity and stability of carbon-supported Pt catalysts.

## 2. Material and methods

### *2.1. Catalysts preparation*

A commercial activated carbon (RGC-30) with a high BET surface area (1598 $m^2/g$) was used as support. The monometallic catalyst, Pt/C, was prepared by impregnating the dry support (383 K, overnight) with an acetone solution (10 mL per gram of support) of $H_2PtCl_6 \cdot 6H_2O$ (Sigma-Aldrich 99.5%) with the appropriate concentration to obtain a Pt loading of 5 wt.%.

After stirring for 12 h, the excess of solvent was slowly evaporated at 313 K under vacuum in a rotary evaporator. Then, the sample was dried at 383 K until complete removal of the solvent.

Bimetallic PtSn catalysts were prepared by sequential impregnation. Tin addition to the dried Pt/C sample was carried out using the proper amount of $SnCl_2$ (99%, Sigma-Aldrich) dissolved in acetone (10 mL of solution per gram of solid) to obtain Pt:Sn atomic ratios of 50:1, 10:1, 1:1, 1:5. After stirring for 12 h, the solvent was removed under vacuum at 313 K. In this way five catalysts were prepared, which were labelled as Pt/C, Pt-Sn/C (50:1), Pt-Sn/C (10:1), Pt-Sn/C (1:1) and Pt-Sn/C (5:1).

### *2.2 Catalysts characterization*

The Pt content of Pt/C and Pt-Sn/C catalysts was determined by burning off the catalysts in air at 1073 K and analysing the residue (dissolved in aqua regia) by ICP-OES (Perkin Elmer, Optima 4300 DV). Temperature-programmed reduction (TPR) with $H_2$ measurements were carried out on the fresh (dried) catalysts in a U-shaped quartz cell using a 5% $H_2$/He gas flow of 50 mL/min, with a heating rate of 10 $K \cdot min^{-1}$. Before the TPR run, the catalyst were pre-treated with flowing He (50 mL/min) at 423 K for 1 h. Hydrogen consumption was followed by on-line mass spectrometry (Pfeiffer, OmniStar GSD 301). X-Ray photoelectron spectroscopy (XPS) analyses were performed with a VG-Microtech Multilab 3000 spectrometer equipped with a hemispherical electron analyser and a Mg-$K_\alpha$ ($h$ = 1253.6 eV; 1 eV = $1.6302 \cdot 10^{-19}$ J) 300 W X-ray source. The powder samples were pressed into small Inox cylinders. Before recording the spectra, the samples were maintained in the analysis chamber until a residual pressure of ca. $5 \times 10^{-7}$ $N \cdot m^{-2}$ was reached. The spectra were collected at pass energy of 50 eV. The intensities were

estimated by calculating the integral of each peak, after subtracting the S-shaped background, and by fitting the experimental curve to a combination of Lorentzian (30%) and Gaussian (70%) lines. The binding energy (BE) of the C l s peak of the support at 284.6 eV was taken as an internal standard. The accuracy of the BE values is ± 0.2 eV. Samples were reduced "*ex-situ*" in flowing $H_2$ for 2 h at 523 K and conserved in octane before the analysis. Conventional TEM analysis was carried out with a JOEL model JEM-210 electron microscope working at 200 kV and equipped with a INCA Energy TEM 100 analytical system and a SIS MegaView II camera. Samples for analysis were suspended in methanol and placed on copper grids with a holey-carbon film support. Catalysts were analysed before (samples reduced at 523 K, 2h) and after being used in the glycerol steam reforming reaction.

### *2.3 Catalytic tests*

The catalytic behaviour of the prepared catalysts in the glycerol steam reforming reaction was evaluated under mild and harder reaction conditions in a fixed bed reactor (Microactivity Refererence). Prior to the activity test, catalysts were *in-situ* reduced under 50mL/min of $H_2$ at 523 K during 2 h. Then, the $H_2$ stream was changed to He, and the temperature was risen up to that of the reaction test, 623 or 673 K. The reaction was carried out at atmospheric pressure, with a feeding (0.05 mL/min) containing 10 or 30% w/w glycerol in water. This 10% w/w glycerol feed composition is similar to that of the glycerol residue obtained from the biodiesel production process after alcohol removal and acid neutralization of the glycerol fraction. Activity tests were performed using 0.200 g of catalyst diluted with SiC, to avoid thermal effects. The composition of the gas stream exiting the reactor was determined by gas chromatography (Agilent

Technologies), with two columns (Carboxen-1000 and Porapak-Q) and two detectors (FID and TCD).

The catalytic performance was evaluated in terms of conversion into gaseous products (based on a carbon balance between the inlet and the outlet of the reactor), selectivity to main reaction products (where "i" is $CO_2$, CO and $CH_4$) and also hydrogen yield, which were defined as:

$$\%\,\text{Conversion} = \frac{\text{C in the gas products}}{\text{C fed into reactor}} \cdot 100$$

$$\%\,\text{"i" selectivity} = \frac{\text{"i" produced experimentally}}{\text{C atoms in the gas products}} \cdot 100$$

$$\%\,H_2\,\text{Yield} = \frac{H_2\ \text{produced experimentally}}{H_2\,\text{calculated according to Eq (1)}} \cdot 100$$

## 3. Results and discussion

### *3.1 Chemical analysis*

Table 1 presents the results of ICP analysis of the Pt content of the different catalysts. It can be seen that the actual metal loading is very close to the nominal one in all cases, this evidencing the efficiency of the impregnation method. Unfortunately, the analysis method used did not allow for the determination of the Sn content due to the volatility of the $SnCl_4$ formed during the digestion process. Thus, these values were estimated by XPS analysis.

### *3.2 X-ray photoelectron spectra (XPS)*

The binding energies of the Pt $4f_{7/2}$ and Sn $3d_{5/2}$ levels for the catalysts reduced in flowing hydrogen at 523 K for 2 h are reported in Table 1. XPS results show that Pt is completely reduced in all the catalysts, as the spectra show only one peak centred at 71.3 eV, which is assigned to metallic Pt. It is noteworthy to mention that a small shift to lower binding energies can be observed in the PtSn/C catalysts compared to the monometallic Pt/C catalyst. This shift may indicate the formation of Pt-Sn alloy phases, as the differences in electronegativity of Pt and Sn could lead to charge transfer from the less-electronegative Sn to the more-electronegative Pt [19,20]. In fact, the analysis of the Sn $3d_{5/2}$ level indicates the presence of two contributions (Table 1). The first one, centred at a binding energy around 486.2-486.4 eV, is assigned to oxidized tin species, Sn(II, IV), and the second one, at around 485.2 eV, corresponds to metallic tin (Sn(0)) [21]. Thus, the presence of metallic tin in the catalysts reduced at 523 K opens up the possibility for the existence of Pt-Sn alloy phases after this treatment, although this cannot be readily assessed by XPS [22,23]. It has also to be taken into account that the use of a relatively inert support such as carbon decreases the possibility of a strong interaction between the tin precursor and the support, this facilitating the Pt-Sn interaction and the formation of Pt-Sn alloy phases [24]. Results obtained for the Pt/Sn atomic ratios are also presented in Table 1. They confirm that the intended amount of tin has been deposited.

### *3.3 Transmission electron microscopy (TEM)*

Fig. 1 shows the TEM images of all samples, before and after being used in the glycerol steam reforming reaction (623 K, 1 atm, 10% w/w glycerol). It can be seen that before the

reaction, (left column) platinum and tin particles are well dispersed on the carbon support, with a homogeneous distribution of the active phase over the catalyst's surface and no agglomerations being observed. It is important to point out that it was not possible to distinguish between Pt and Sn, as both species appear in the images as dark dots.

TEM micrographs and particle size distribution of all catalyst were also taken after reaction (right column) and some agglomerations can be observed in this case. It can be seen that a considerable sintering of the metal particles has been produced to different extents depending on the sample. In this way, it is noteworthy to note that agglomerations in the tin-containing catalysts are less evident than in the monometallic Pt/C catalyst, and a lesser amount of agglomerates are formed when the amount of tin in the catalyst is increased. This indicates that Sn provides a stabilizing effect on the Pt particles avoiding their sintering, as it has also been observed in other works [15,25]. Under these conditions, the presence of coke is not observed. It is well known that Sn inhibits the reactions leading to the formation of coke precursors, and improves in this way the stability of the catalysts under reaction conditions [24].

### *3.4 Temperature programmed reduction*

Fig. 2 shows the TPR profiles of the carbon-supported Pt-Sn catalysts after the drying process. The TPR profile of the carbon support only shows one $H_2$ consumption peak at high temperature (800-1100 K). This peak appears in all the catalysts, and it has been attributed to the reaction of $H_2$ with reactive surface sites created by decomposition of surface functional groups (mainly those that evolve as CO) on the support [26]. For the monometallic Pt/C catalyst three $H_2$ consumption peaks can be clearly observed. The first one (400-500 K) is assigned to the

reduction of the impregnated metal chloride complex to form metallic Pt particles; the second one, at intermediate temperatures (490-590 K), can be attributed to $H_2$ consumption by oxygen surface functionalities present on the support. Hydrogen which is previously chemisorbed and dissociated on Pt particles is transported to the carbon surface by spillover, where it reacts with the oxygen groups located at the metal-carbon interface [27]. The third peak at higher temperatures (773-873 K) is attributed to hydrogen consumption by the reduction of oxygen superficial groups on the carbon support that are not located near the metal particles.

On the other hand, the $H_2$-TPR profiles for the bimetallic catalysts differ as the amount of tin is increased. The peak at low temperatures becomes more pronounced with the increase of the amount of tin. The reduction profile of Pt-Sn/C (50:1) is very similar to that of the Pt/C catalyst. The increase of the amount of Sn produces a more intense peak due to the reduction of both platinum and tin precursors, this revealing the close proximity and strong interaction between both species. Thus, tin is reduced at lower temperature due to the presence of platinum in the catalysts [28,29]. The observed reduction process at intermediate temperatures can be attributed to the reduction of oxidised Sn species (Sn(II) and/or Sn(IV)) that are not in intimate contact with Pt. Interestingly, no high temperature reduction peaks are observed in these profiles, what can be due to the partial blockage/decomposition of the oxygen surface groups during the impregnation with the tin precursor and drying.

Based on the reduction profiles shown, and considering that the reduction treatment applied previously to the reforming reaction is carried out at 523 K, we can assume that the bimetallic catalysts are, before reaction, composed of metallic Pt, a fraction of oxidized tin species (Sn (II)/Sn (IV)) and metallic Sn, likely forming alloy phases with Pt. This conclusion is also supported by XPS data (Table 1).

### *3.5 Catalytic behaviour*

The catalytic behaviour of the prepared catalysts in terms of gas phase conversion as a function of time on stream, after being reduced at 523 K, is reported in Fig. 3. The steam reforming of glycerol was performed at atmospheric pressure, 623 K and 0.05 mL/min of a 10% w/w of aqueous glycerol solution. The gas phase analysis was carried out every 30 min by on line chromatography. The results presented are the average of three experiments with very good reproducibility (error of ±3%). A blank run without catalyst was also performed, and negligible glycerol conversion was obtained.

The gas phase conversions, after an initial increase during the first 2-3 h on stream, were stable during the period of time studied (7.5 h). For the monometallic catalyst, Pt/C, and the bimetallic catalysts with low tin content (Pt-Sn/C (50:1) and Pt-Sn/C (10:1)) the conversion was complete, with all the glycerol solution being transformed to gaseous products. A decrease of the gas phase conversion was observed with the increase of the tin content in the samples. For Pt-Sn/C (1:1) the conversion was about 78%, and for the catalyst with the highest Sn content (Pt-Sn/C (1:5)) the conversion was very low, about 10%. This low conversion may be due to excessive blocking of the active sites of Pt by the large amount of Sn present. In fact, a certain free adjacent active sites of Pt are needed to adsorb and activate the glycerol molecule (cleavage of C-C bond) so that it can be reformed [30]. In addition, the differences in metal particle sizes (Fig. 1) have also an effect on the activity of the samples. For the optimum amount of Sn, Pt particles are stabilised thus avoiding their sintering and resulting in a greater Pt particles dispersion. The later means higher active sites available for the adsorption of glycerol molecules on the metallic surface and its subsequent reforming. As can be seen in Figure 3, the activity was higher for the catalysts with low tin content.

The composition of the gas phase product stream is reported in Table 2. These results were obtained when the conversion reached a stable value, after 5 h on stream. It can be observed in Table 2 that the $H_2$/CO molar ratio is close to 1 for the monometallic catalyst and for the bimetallic catalysts with low Sn contents. For the samples with higher Sn content an increase of this ratio was observed, reaching a value of 3.56 for the Pt-Sn/C (1:5) catalyst. Furthermore, the CO/$CO_2$ molar ratio tends to decrease with increasing the amount of tin in the catalysts.

These results point to an enhancement of the water-gas shift reaction, which would be favoured by tin species. There are few reports in the literature on the role of Sn in the water-gas shift reaction. Recently, Gupta and Hegde reported the catalytic behaviour of a $Ce_{0.78}Sn_{0.2}Pt_{0.02}O_{2-\delta}$ catalyst, which was able to convert over 99.5% CO to $H_2$ at 573 K [31]. In this case, the role of tin species was claimed to be the stabilization of the catalyst surface against the formation of deactivating carbonate species. On the other hand, Azzam *et al.* studied the role of the support in Pt-based catalysts for water gas shift [32], including a titania-supported bimetallic 0.5%Pt-0.3%Sn catalyst. Although it was less active than other catalysts studied, such as Pt-Re/$TiO_2$, it showed a high catalytic stability at 573 K.

Values for the $CH_4$/$H_2$ molar ratio in Table 2 show that methane formation is very low for all catalysts. In fact, nearly no methane was produced by the catalyst with the highest amount of tin, Pt-Sn/C (1:5). The low methane formation is indicative of the role of tin in inhibiting hydrogenation reactions between CO/$CO_2$ and the $H_2$ formed [15].

The $H_2$, CO, $CO_2$ and $CH_4$ selectivities (after 5 hours of reaction, time when catalytic activity is stable) are presented in Fig. 4. The effect of tin is clearly observed. The $CO_2$ selectivity slightly increases with the amount of Sn while the CO selectivity decreases. This

change is more pronounced with the Pt-Sn/C (1:5) catalyst, so the Sn addition in large amounts promotes the CO oxidation producing $H_2$-rich gas streams and not streams for syngas. Furthermore the $H_2$ selectivity increases with Sn addition except for the catalyst with the highest amount of Sn, but this could be explained as due to the low conversion to gas phase and the possible $H_2$ consumption in the formation of liquid products.

Finally, considering the above results a stability test (not shown) was carried out with the Pt/C and Pt-Sn/C (1:1) catalysts, in order to determining the effect of tin during longer reaction (24 hours) in the same temperature conditions (623 K). In both cases, the conversion to gas phase products remained stable during all the experiment.

In view of these results, it was decided to test these catalysts under harder reaction conditions: higher temperature (673 K) and a more concentrated of glycerol feed solution (30% w/w glycerol in water). The results of these experiments are shown in Fig. 5.

Under these conditions the monometallic Pt/C was nearly inactive, producing only about 5% conversion in the first hour on stream. In contrast, for the bimetallic catalyst Pt-Sn/C (1:1) the conversion decreased with respect to reaction under milder reaction conditions (78% versus 50%), but an excellent performance stability, for almost 10 hours on stream, was obtained under these harder reaction conditions. Furthermore, the $H_2$, CO, $CO_2$, $CH_4$ selectivities and $H_2$ yield for PtSn(1:1)/C are presented in Figure 6. Despite the lower conversion in these conditions, $H_2$ selectivity remains high with low methane formation.

The formation of coke is favoured at high reaction temperature and with high glycerol concentration in the feed stream. This fact can explain the fast deactivation of the Pt/C catalyst, which showed a good activity and stability under milder reaction conditions. It is well known

that Sn is able to inhibit coke formation reactions in processes such as the dehydrogenation of hydrocarbons [24]. Thus, by electronic and/or geometric effects Sn is able to modify the catalytic properties of Pt, inhibiting reactions that form coke precursors and, thereby, improving the stability of the catalyst. The effect of Sn may be similar in the reforming reaction of glycerol. Probably a strong Pt-Sn interaction (as indicated by the results of TPR, Fig. 2) inhibits reactions that produce olefins (coke precursors) during glycerol reforming. Furthermore, Sn has also a textural promoter effect, inhibiting the sintering of Pt particles (as shown by TEM photographs) at these higher reaction temperature conditions. Nevertheless, it has to be taken into account that the beneficial effects of the presence of Sn become detrimental if a too high amount of this promoter is present, as the amount of active Pt surface sites decrease and, thus, the catalytic activity.

## 4. Conclusions

The effect of Sn addition to Pt/C catalyst with different Pt:Sn ratios was investigated in the glycerol steam reforming reaction. XPS and TPR-$H_2$ data revealed the close proximity and strong interaction between Pt and Sn. TEM images showed that metal agglomerations in the tin-containing catalysts were less evident than in the monometallic Pt/C catalyst, and a lesser amount of agglomerates were formed when the amount of tin in the catalyst is increased.

Regarding catalytic tests, a good behaviour in terms of activity and stability was obtained with bimetallic PtSn/C catalysts with low Sn/Pt ratios, both under mild reaction conditions (10 wt% glycerol and 623 K) and under more severe conditions (30 wt% glycerol and 673 K). It was found that Sn promotes the CO oxidation reaction producing $H_2$-rich gas streams. Furthermore,

the $H_2$ selectivity increased with low Sn/Pt ratios. Sn is also able to inhibit coke formation reactions and hinder Pt sintering, thereby improving the stability of the catalyst.

## ACKNOWLEDGMENTS

This work has been supported by Ministerio de Economía y Competitividad (Spain, Project MAT2010-21147). L.P.P. acknowledges her grant BES-2011-0406508.

## REFERENCES

[1] Cortright RD, Davda RR, Dumesic JA. Hydrogen from catalytic reforming of biomass-derived hydrocarbons in liquid water. Nature 2002;418:964-7.

[2] Saxena RC, Adhikari DK, Goya HB. Biomass-based energy fuel through biochemical routes: a review. Renew. Sustain. Energy Rev 2009;13:167-78.

[3] Kim S.M, Woo S.I. Sustainable production of syngas from biomass-derived glycerol by steam reforming over highly stable Ni/SiC. ChemSusChem 2012;5:1513-22.

[4] Melero JA, Vicente G, Paniagua M, Morales G, Muñoz P, Synthesis of oxygenated compounds for fuel formulation: Etherification of glycerol with ethanol over sulfonic modified catalysts. Bioresour. Technol. 2012;103:142-51.

[5] Avasthi KS, Reddy RN, Patel S. Challenges in the production of hydrogen from glycerol - A biodiesel byproduct via steam reforming process. Procedia Eng. 2013;51:423-9.

[6] Soares RR, Simonetti DA, Dumesic JA. Glycerol as a source for fuels and chemicals by low-temperature catalytic processing. Angew. Chem. Int. 2006;45:3982-5.

[7] Davda RR, Shabaker JW, Huber GW, Cortright RD, Dumesic JA. A review of catalytic issues and process conditions for renewable hydrogen and alkanes by aqueous-phase reforming of oxygenated hydrocarbons over supported metal catalysts. Appl. Catal. B: Env. 2005;56:171-86.

[8] Simonetti DA, Hansen R, Kunkes EL, Soares RR, Dumesic JA. Coupling of glycerol processing with Fischer-Tropsch synthesis for production of liquid fuels. Green Chem. 2007;9:1073-83.

[9] Kunkes EL, Soares RR, Simonetti DA, Dumesic JA. An integrated catalytic approach for the production of hydrogen by glycerol reforming coupled with water-gas shift. Appl. Catal. B: Env. 2009;90:693-8.

[10] Piscina PR, Homs N. Use of biofuels to produce hydrogen [reformation processes]. Chem. Soc. Rev. 2008;37:2459-67.

[11] Iriondo A, Barrio VL, Cambra JF, Arias PL, Güemez MB, Navarro RM, et al. Influence of $La_2O_3$ modified support and Ni and Pt active phases on glycerol steam reforming to produce hydrogen. Catal. Comm. 2009;10:1275-8.

[12] Adhikari S, Fernando S, Haryanto A. Production of hydrogen by steam reforming of glycerin over alumina-supported metal catalysts. Catal. Today 2007;129:355-64.

[13] Dauenhauer PJ, Salge JR, Schmidt LD. Renewable hydrogen by autothermal steam reforming of volatile carbohydrates. J. Catal. 2006;244:238-47.

[14] Pompeo F, Santori G, Nichio NN. Hydrogen and/or syngas from steam reforming of glycerol. Study of platinum catalysts. Int. J. Hydrogen Energ. 2010;35:8912-20.

[15] Shabaker JW, Huber GW, Dumesic JA, Aqueous-phase reforming of oxygenated hydrocarbons over Sn-modified Ni catalysts. J. Catal. 2004;222:180-91.

[16] Shabaker JW, Simonetti DA, Cortright RD, Dumesic JA. Sn-modified Ni catalysts for aqueous-phase reforming: Characterization and deactivation studies. J. Catal. 2005;231:67-76.

[17] Sánchez-Sánchez MC, Navarro RM, Fierro JLG. Ethanol steam reforming over $Ni/M_xO_y$-$Al_2O_3$ (M=Ce, La, Zr and Mg) catalysts: Influence of support on the hydrogen production. Int. J. of Hydrogen Energ. 2007;32:1462-71.

[18] Kaya B, Irmak S, Hasanoglu A, Erbatur O. Evaluation of various carbon materials supported Pt catalyts for aqueous-phase reforming of lignocellulosic biomass hydrolysate. Int. J. Hydrogen Energ. 2014;39:10135-40.

[19] Kim JH, Choi SM, Nam SH, Seo MH, Choi SH, Kim WB. Influence of Sn content on PtSn/C catalysts for electrooxidation of $C_1$–$C_3$ alcohols: Synthesis, characterization, and electrocatalytic activity. Appl. Catal. B: Env. 2008;82:89-102.

[20] Siri GJ, Ramallo-López JM, Casella ML, Fierro JLG, Requejo FG, Ferretti OA. XPS and EXAFS study of supported PtSn catalysts obtained by surface organometallic chemistry on metals: Application to the isobutane dehydrogenation. Appl. Catal. A: Gen. 2005;278:239-49.

[21] Wagner CD, Naumkin AV, Kraut-Vass A, Allison JW, Powell CJ, Rumble JR. NIST X-ray Photoelectron Spectroscopy Database, Gaithersburg 2007.

[22] Ruiz-Martínez J, Coloma F, Sepúlveda-Escribano A, Anderson JA, Rodríguez-Reinoso F. Effect of tin content and reduction temperature on the catalytic behaviour of $PtSn/TiO_2$ catalysts in the vapour-phase hydrogenation of crotonaldehyde. Catal. Today 2008;133:35-41.

[23] Coloma F, Sepúlveda-Escribano A, Fierro JLG, Rodríguez-Reinoso F. Crotonaldehyde hydrogenation over bimetallic Pt-Sn catalysts supported on pregraphitized carbon black. Effect of the preparation method. Appl. Catal. A: Gen. 1996;148:63-80.

[24] Serrano-Ruiz JC, Sepúlveda-Escribano A, Rodríguez-Reinoso F. Bimetallic PtSn/C catalysts promoted by ceria: Application in the nonoxidative dehydrogenation of isobutane. J. Catal. 2007;246:158-65.

[25] Lima SM, Silva AM, Jacobs G, Davis BH, Mattos LV, Noronha FB. New approaches to improving catalyst stability over Pt/ceria during ethanol steam reforming: Sn addition and $CO_2$ co-feeding. Appl. Catal. B: Env. 2010;96:387-98.

[26] Miguel SR, Scelza OA, Román-Martínez MR, Salinas-Martínez de Lecea C, Cazorla-Amorós D, Linares-Solano A. States of Pt in Pt/C catalyst precursors after impregnation, drying and reduction steps. Appl. Catal. A: Gen. 1998;170-93.

[27] Miguel SR, Román-Martínez MC, Jablonski EL, Fierro JLG, Cazorla-Amorós D, Scelza OA. Characterization of Bimetallic PtSn Catalysts Supported on Purified and $H_2O_2$-Functionalized Carbons Used for Hydrogenation Reactions. J. Catal. 1999;184:514-25.

[28] Román-Martínez MC, Cazorla-Amorós D, Miguel SR, Scelza OA. Carbon-supported PtSn catalysts: Characterization and catalytic properties. J. Jpn. Petrol. Inst. 2004;47:164-78.

[29] Arteaga G, Medina A, Colina O, Rodríguez D, Domínguez F, Sánchez J. Efectos de la adición de Li y K sobre las propiedades catalíticas de los catalizadores de $Pt/Al_2O_3$ y $Pt-Sn/Al_2O_3$ en la deshidrogenación de n-butano. Ciencia 2008;16:354-64.

[30] Lamy C, Coutanceau C. Catalysts for Alcohol-Fuelled Direct Oxidation Fuel Cells ed. Zhen-Xing Liang Tim S. Zhao RSC Energy and Environment Series No.6 2012.

[31] Gupta A, Hegde MS. $Ce_{0.78}Sn_{0.2}Pt_{0.02}O_{2-\delta}$: A new non-deactivating catalyst for hydrogen production via water-gas shift reaction. Appl. Catal. B: Env. 2010;99:279-88.

[32] Azzam KG, Babich IV, Seshan K, Lefferts L. A bifunctional catalyst for the single-stage water–gas shift reaction in fuel cell applications. Part 2. Roles of the support and promoter on catalyst activity and stability. J. Catal. 2007;251:163-71.

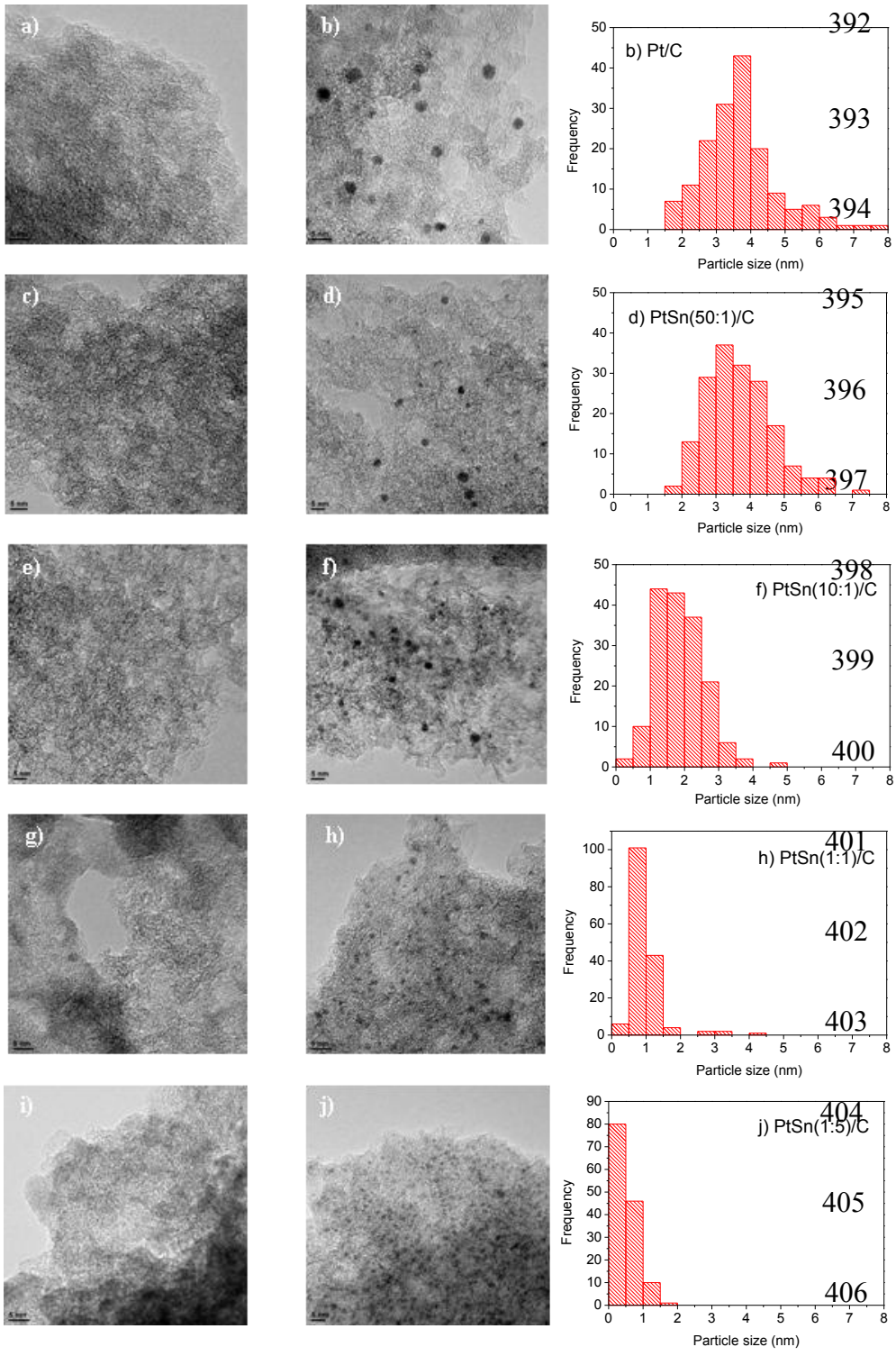


407 **Figure 1**. TEM images before (left column) and after glycerol steam reforming (right column)
408 for a), b) Pt/C; c), d) Pt-Sn/C (50:1); e), f) Pt-Sn/C (10:1); g), h) Pt-Sn/C (1:1) and i), j) Pt-Sn/C
409 (1:5) catalysts and particle size distributions for all catalysts after glycerol steam reforming.

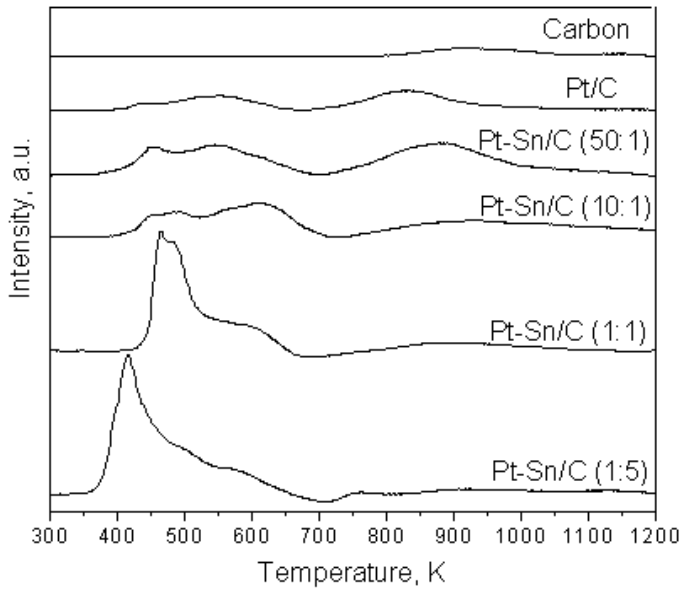


410

411 **Figure 2**. $H_2$-TPR profiles for the fresh dried catalysts.

412

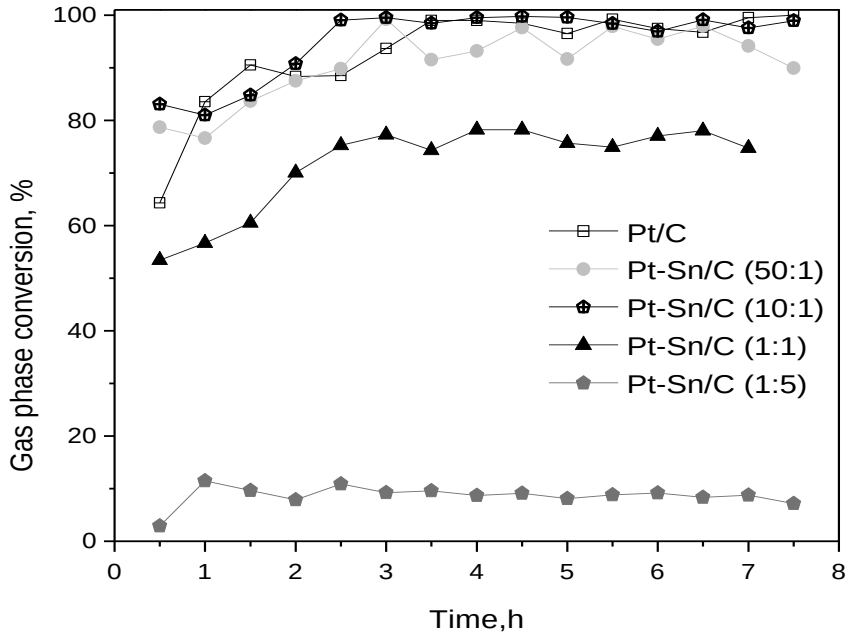


413

414 **Figure 3.** Gas phase conversion vs. time on stream of the different catalysts in glycerol steam

415 reforming at 623 K.

416

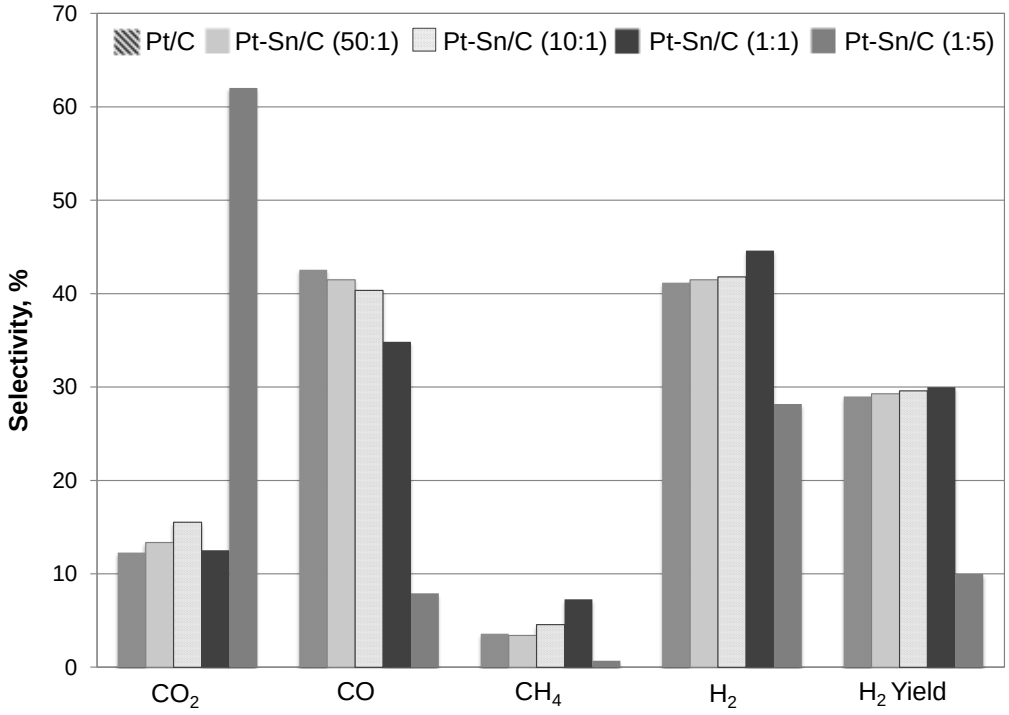


417

418 **Figure 4**. Selectivity for the gaseous products in the GSR at 623 K.

419

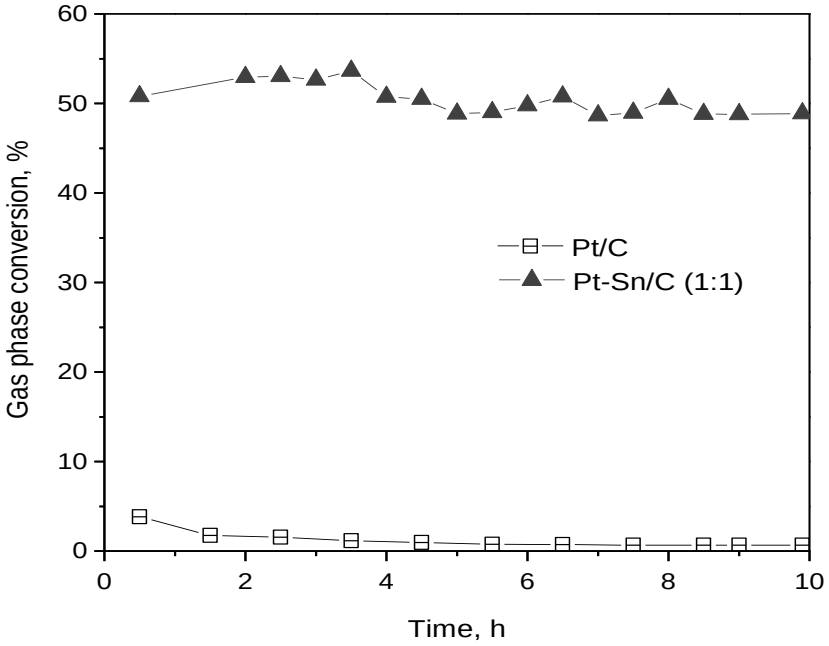


420

421 **Figure 5.** Gas phase conversion vs time of reaction for Pt/C and Pt-Sn/C (1:1) catalysts at 673 K

422 and feed of 30 % w/w of glycerol.

423

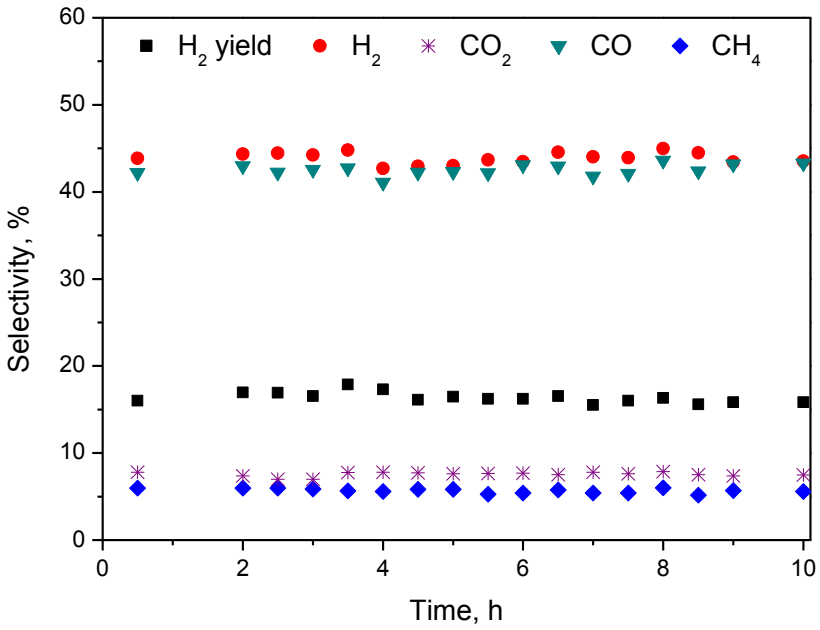


**Figure 6**. Selectivity for the gaseous products and $H_2$ yield for Pt-Sn/C (1:1) catalyst at 673 K and feed of 30 % w/w of glycerol.

428 **Table 1.** Atomic ratios and binding energies of the Pt $4f_{7/2}$ and Sn $3d_{5/2}$ levels in catalysts
429 reduced at 523 K, and Pt loading.

| Catalyst | Binding energies (eV) | | Sn(0)/[Sn(II,IV)+Sn(0)] | Pt/Sn (at/at) | *Pt (wt.%) |
|---|---|---|---|---|---|
| | Pt $4f_{7/2}$ | Sn $3d_{5/2}$ | | | |
| **Pt/C** | 71.4 | -- | | -- | 4.8 |
| **Pt-Sn/C (50:1)** | 71.3 | 485.2 - 486.4 | 0.048 | 46.3 | 4.9 |
| **Pt-Sn/C (10:1)** | 71.3 | 485.2 - 486.3 | 0.107 | 11.4 | 4.8 |
| **Pt-Sn/C (1:1)** | 71.3 | 485.2 - 486.2 | 0.086 | 0.87 | 4.6 |
| **Pt-Sn/C (1:5)** | 71.2 | 485.2 - 486.3 | 0.074 | 0.28 | 4.7 |

430 * Determined by ICP analysis.

431

**Table 2**. Phase gas composition (molar ratios) and conversion in glycerol steam reforming at 623 K for all samples.

| Catalyst | $H_2/CO$ | $CO/CO_2$ | $CH_4/H_2$ | Gas phase conv. (%) |
|---|---|---|---|---|
| Pt/C | 0.97 | 3.46 | 0.09 | 100 |
| Pt-Sn/C (50:1) | 1.00 | 3.10 | 0.08 | 98 |
| Pt-Sn/C (10:1) | 0.98 | 2.60 | 0.12 | 100 |
| Pt-Sn/C (1:1) | 1.28 | 2.78 | 0.16 | 78 |
| Pt-Sn/C (1:5) | 3.56 | 0.13 | 0.01 | 9 |